Article

Cyclic Carbonates through the Photo-Induced Carboxylative Cyclization of Allylic Alcohol with CO_2: A Comprehensive Kinetic Study of the Reaction Mechanism by In Situ ATR-IR Spectroscopy

Joseph Grondin, Christian Aupetit, Jean-Marc Vincent and Thierry Tassaing *

Institut des Sciences Moléculaires, UMR 5255 CNRS, Université de Bordeaux, 351, Cours de la Libération, F-33405 Talence, France; joseph.grondin@u-bordeaux.fr (J.G.); christian.aupetit@u-bordeaux.fr (C.A.); jean-marc.vincent@u-bordeaux.fr (J.-M.V.)
* Correspondence: thierry.tassaing@u-bordeaux.fr

Abstract: A one-pot multicomponent green process is investigated for the synthesis of perfluoroalkylated cyclic carbonate which merges the photo-promoted Atom Transfer Radical Addition (ATRA) of a perfluoroalkyl iodide (Rf-I) onto allyl alcohols with the Lewis-base-promoted carboxylative cyclization. The evolution of the complex mixture during the reaction was monitored by in situ ATR-IR and Raman spectroscopies that provided insights into the reaction mechanism. The effect on the kinetics and the carbonate yields of key parameters such as the stoichiometry of reagents, the nature of the Lewis base and the solvent, the temperature and the pressure were evaluated. It was found that high yields were obtained using strong Lewis bases that played both the role of activating the allyl alcohol for the generation of the allyl carbonate in the presence of CO_2 and promoting the ATRA reaction through the activation of C_4F_9I by halogen bonding. This protocol was also extended to various unsaturated alcohols.

Keywords: CO_2 organocatalysis; photo-promoted ATRA; cyclic carbonates

1. Introduction

During the last decade, much academic and industrial research has been devoted to the development of sustainable synthetic pathways to produce five membered cyclic carbonates by the catalytic coupling of CO_2 with epoxides [1–5] using appropriate organic or transition metal catalysts. This 100% atom economic reaction is very attractive as it represents a greener and safer alternative to the conventional synthesis of cyclic carbonates from diols and toxic phosgene. Today, these precursors find applications as electrolytes in Li-ion batteries, intermediates for fine chemical synthesis and polar aprotic solvents replacing DMF, DMSO, NMP and acetonitrile [6]. They also serve as raw materials for the synthesis of polycarbonates [7,8] and isocyanate-free polyurethanes [9–12] (NIPUs) that become more and more attractive for the industry as an alternative to classical polyurethanes (PUs). In view of the broad scope of applications of cyclic carbonates and their strong economic potential, there is still a need to improve their synthesis and decrease their production costs. In particular, whereas the synthesis of terminal cyclic carbonates from the coupling of CO_2 with epoxides is well established, the conversion of internal tri- and tetra-substituted epoxides into their corresponding five-membered carbonates is still very challenging even though of great interest [13]. On the other hand, the synthesis of six-membered cyclic carbonates by oxetane/CO_2 coupling [13–15] remains challenging because of (i) the lower reactivity of four-membered ether rings compared to epoxides even under harsh experimental conditions, and (ii) a poor reaction selectivity. Interestingly, α-alkylidene cyclic carbonates that are synthesized by coupling CO_2 with propargylic alcohols using organocatalysts or metal-based catalysts are intermediates of the great

interest in organic and polymer synthesis [16–24]. However, at present, the substrate scope is mainly restricted to tertiary alcohols as only few examples are reported using primary and secondary alcohols [25–27]. Finally, 1,2 and 1,3-diols [28–32] were subjected to carbonation in order to afford five- and six-membered cyclic carbonates, respectively, but their reaction with CO_2 is limited due to the formation of water as a by-product. To circumvent this drawback, both homogeneous and heterogeneous catalysts (Bu_2SnO, K_2CO_3, CeO_2, etc.) used in combination with dehydrating systems were developed [33,34]. Although one efficient system involving CeO_2 as the catalyst and 2-Cyanopyridine as dehydrating agent has been developed [34], this process requires harsh reaction conditions (150 °C, 5 MPa) and a large excess of an expensive dehydrating agent. Alternative protocols have been recently suggested to overcome the limitation induced by the formation of water by combining the use of an organic base and an alkylating agent under mild conditions. For example, Zhang et al. [35] and Buchard et al. [36,37] have combined strong Lewis bases and Tosyl chloride (TsCl) as the alkylating agent to promote the synthesis of six-membered cyclic carbonates. A similar strategy has been proposed by Kitamura et al. [38] and Dyson et al. [31] using alkyl halides as the alkylating agents for the synthesis of cyclic carbonates. The effect of the addition of ionic liquids to these systems to obtain cyclic carbonates from diols was also investigated [39]. A critical assessment of the reaction mechanism at work in such metal-free dual activating systems for the coupling of CO_2 with 1,x-diols to afford (a) cyclic carbonates has been recently proposed by Brege et al. [40]. In particular, it was shown that after choosing either DBU/EtBr or TEA/TsCl as the organic dual activating system, it was possible to control the product selectivity to substituted cyclic and/or acyclic carbonates depending on the nature of the substrate. Therefore, there is still a need to develop innovative routes to broaden the structural diversity of cyclic carbonates that could be exploited for the design of novel functionalized chemicals and polymers.

In this context, light-driven CO_2 fixation through C–C bond formation to produce added value chemicals and monomers remains a relatively unexplored area, although it represents a very promising field and an attractive green route [41–45].

A recent review reports several typical examples on the photochemical fixation of CO_2 into heterocyclic scaffolds with detailed mechanistic descriptions of the various proposed synthetic routes [46]. For example, an original radical synthetic route was proposed for the synthesis of oxazolidinones through the photopromoted base-catalyzed coupling of CO_2 with allylamines [43] or propargyl amines [47] in the presence of perfluoroalkyl iodides and iodine, respectively. In the work by Wang et al. [43], allyl alcohols were investigated to a limited extent, although the reaction could be very useful for the preparation of cyclic carbonates. In addition, the proposed mechanism was supported by a few mechanistic experiments conducted mostly using ^{1}H NMR. Very recently, Jain et al. reported the first photochemical synthesis of linear carbonates from the reaction of CO_2 with alcohols using a silver-doped ceria nanocomposite at room temperature under visible light irradiation [48]. In this context, we decided to investigate the synthesis of cyclic carbonates through a one-pot multicomponent metal-free process which merges the photo-promoted Atom Transfer Radical Addition (ATRA) of a perfluoroalkyl iodide (Rf-I) onto unsaturated alcohols with the Lewis-base-promoted carboxylative cyclization (Scheme 1). A detailed in situ ATR-IR and Raman spectroscopic study led to the optimization of reaction conditions and provided insights into the reaction mechanism. In addition, the stoichiometry of reagents, the nature of the Lewis base, the effects of the temperature, the pressure and the solvent on the kinetics and the carbonate yields were evaluated. Finally, using optimized conditions, the carbonation scope was extended to a variety of unsaturated alcohol substrates.
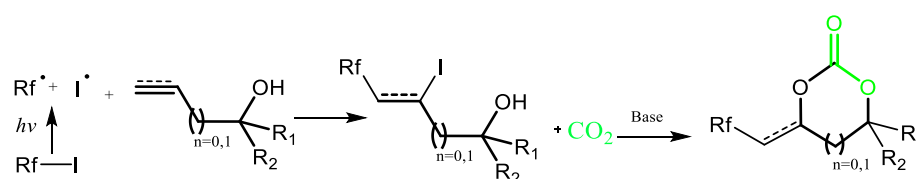
Scheme 1. Proposed synthesis of 5–6-membered cyclic carbonates through a photo-promoted ATRA reaction followed by a Lewis-base-promoted carboxylative cyclization. The color of green puts in evidence the position of CO_2 in the final product.

2. Results and Discussion

2.1. Synthesis of Perfluorobutyl Cyclic Carbonate 1 from the Coupling of CO_2 with Allylic Alcohol and Perfluorobutyliodide: Mechanistic Study

2.1.1. Model Reaction Using Allyl Alcohol, DBU and C_4F_9I

An in situ ATR-IR/Raman kinetic study for the preparation of carbonate **1** was first performed under UVA irradiation at 365 nm (LED) in the presence of 1,8-diazabicyclo-[5.4.0]-undec-7-ene (DBU), perfluorobutyl iodide (C_4F_9I) and allyl alcohol. The reaction was conducted in acetonitrile (CH_3CN) at T = 25 °C under a low carbon dioxide pressure of 0.3 MPa (Scheme 2) using a slight excess of DBU (1.05 equiv.) and C_4F_9I (1.25 equiv.) relative to allyl alcohol.
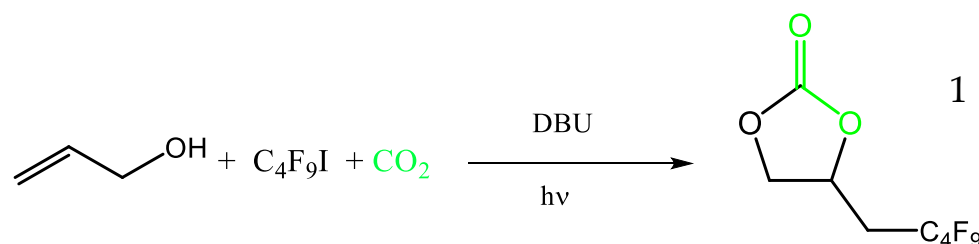
Scheme 2. Benchmark reaction for the synthesis of the perfluorobutyl carbonate **1**. $DBUH^+$-I^- is obtained as a by-product. The color of green puts in evidence the position of CO_2 in the final product.

Typical ATR-IR spectra of the mixture obtained at different reaction times are depicted in Figure 1, where specific spectral signatures of reactants, intermediates and products could be identified. From the spectrum of the reaction mixture before the addition of CO_2, we have identified specific peaks of interest.
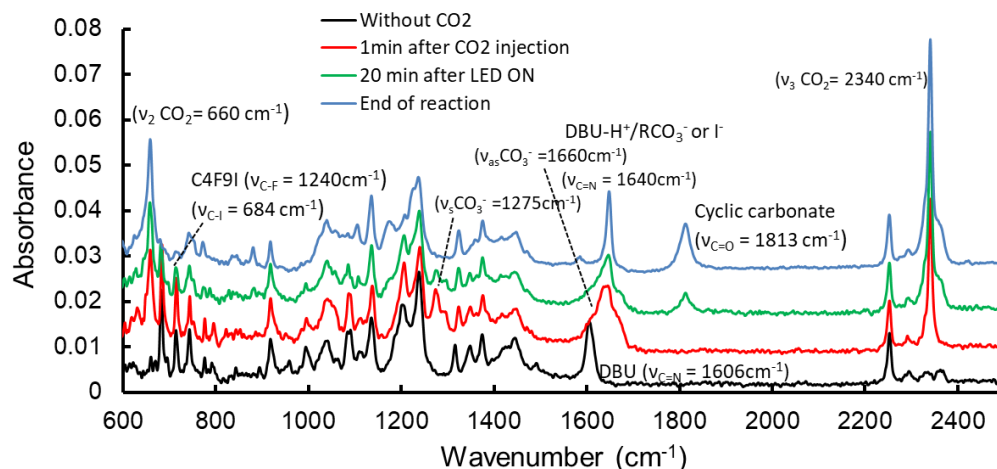

Figure 1. ATR-IR spectra of the reaction medium at several times during the reaction. Conditions: allyl alcohol (48 μL, 0.5 mmol), DBU (1.05 equiv.), C_4F_9I (1.25 equiv.), CH_3CN (1 mL), 25 °C, CO_2 (0.3 MPa), irradiation at 365 nm (LED) under stirring.

Before the addition of CO_2 to the ternary mixture of allyl alcohol, DBU and C_4F_9I, a narrow band is observed at 1606 cm^{-1} that is characteristic of the C=N stretching mode of DBU, indicating that there is no specific interaction and/or reaction between DBU and another reactant of the mixture (black curve). In particular, there is no deprotonation of the alcohol moiety by DBU, as well as no alkylation of DBU by C_4F_9I. We have also identified a peak at 684 cm^{-1} that is assigned to a C-I stretching mode coupled with the C−F bending modes of C_4F_9I. Unfortunately, we do not detect any contribution of the allyl alcohol. After the addition of CO_2 at a pressure of 0.3 MPa (red curve), the DBU absorption band shifts at 1642 cm^{-1}, which has been assigned to the C=NH$^+$ stretching mode of protonated DBU [40,49]. Concomitantly, a shoulder of this broad peak appears around 1660 cm^{-1}, as well as a new peak at 1275 cm^{-1}, both being attributed to C−O stretching modes of the allyl carbonate anion CH_2=$CHCH_2CO_3^-$ [50]. Thus, in the dark, a trimolecular reaction between CO_2, allyl alcohol and DBU occurs, which leads to the formation of the organic salt CH_2=$CHCH_2CO_3^-$/DBUH$^+$. We emphasize that the peak of DBU is barely detected as a shoulder at about 1606 cm^{-1}; its intensity provides an estimated concentration between 0.05 and 0.1 equiv. of DBU still present in the mixture under these experimental conditions that is consistent with the thermodynamic data of Heldebrant et al. [51]. Therefore, the allylic alcohol is quantitatively transformed into its carbonated form during this first step of the reaction that occurs within 5 min as it is mainly controlled by CO_2 solubilisation kinetic in the organic phase. Then, when the LED is switched ON and during the course of the kinetic (green and blue curves), the main absorption of DBUH$^+$ is slightly shifted toward higher wavenumbers from 1642 cm^{-1} to 1648 cm^{-1}; it becomes thinner as the shoulder tends to disappear due to the carbonate anion. The slight shift is ascribed to anion metathesis of DBUH$^+$/RCO$_3^-$ to DBUH$^+$/I$^-$ that should occur upon carbonate cyclization (Scheme 1). Accordingly, the characteristic peak of RCO$_3^-$ at 1275 cm^{-1} becomes weaker as a function of time. Concomitantly, the new absorption band at 1813 cm^{-1}, assigned to the C=O stretching mode of the perfluoroalkylated cyclic carbonate, smoothly increases with time. In the same time, the band at 684 cm^{-1} associated with C_4F_9I vanishes at the end of the reaction. We emphasize that the intermediate ATRA product with the formation of a C-I bond was not detectable in our experimental conditions as the C-I stretching mode is observable by ATR-IR at wavenumbers lower than 600 cm^{-1}. Thus, the rate of the concentration evolution of C_4F_9I, RCO$_3^-$, and the cyclic carbonate could be monitored by ATR-IR from the height of the peak at 684 cm^{-1}, 1275 cm^{-1} and 1813 cm^{-1}, respectively. To obtain the complementary information from the allyl function of the alcohol that is not detectable by ATR-IR, the kinetic of the same model reaction was monitored by in situ Raman spectroscopy in order to follow the evolution of the height of the peak at 1645 cm^{-1} characteristic of the C=C bond of the allyl alcohol (or allyl carbonate anion at the same wavenumber) and that of cyclic carbonate observed at 1813 cm^{-1} (see ESI Figure S1).

Figure 2 displays the kinetic profiles of the disappearance of the C_4F_9I substrate and allyl carbonate intermediate generated quantitatively before irradiation, as well as of the appearance of the cyclic carbonate product **1**. For comparison, the kinetic profiles of the cyclic carbonate bands measured in Raman and ATR-IR have been scaled to their maximum intensity at 600 min. By the same token, the maximum of the kinetic profile at t = 0 of the C=C and RCO$_3^-$ band have been scaled at about the maximum peak height of the C_4F_9I band. Good agreement is observed between the IR and Raman follow-ups of the cyclic carbonates, thus validating the repeatability of our experimental procedure. The profiles show that the reaction is completed in about 8 h, time after which the reagents have been fully consumed, while the cyclic carbonate **1** is formed with a yield of >95% as determined by ATR-IR using Equation (1) in Section 3.2. The reaction thus occurs with an excellent selectivity. The ATRA process is supported by the smooth decrease in the intensity of the Raman band assigned to the C=C stretching mode of the allyl carbonate. Interestingly, the kinetic profiles reveal that the rates of formation of **1** and consumption of the allyl carbonate and C_4F_9I occur with the same rates, thus showing that the rate of the intramolecular cyclization is much higher than that of the ATRA process.
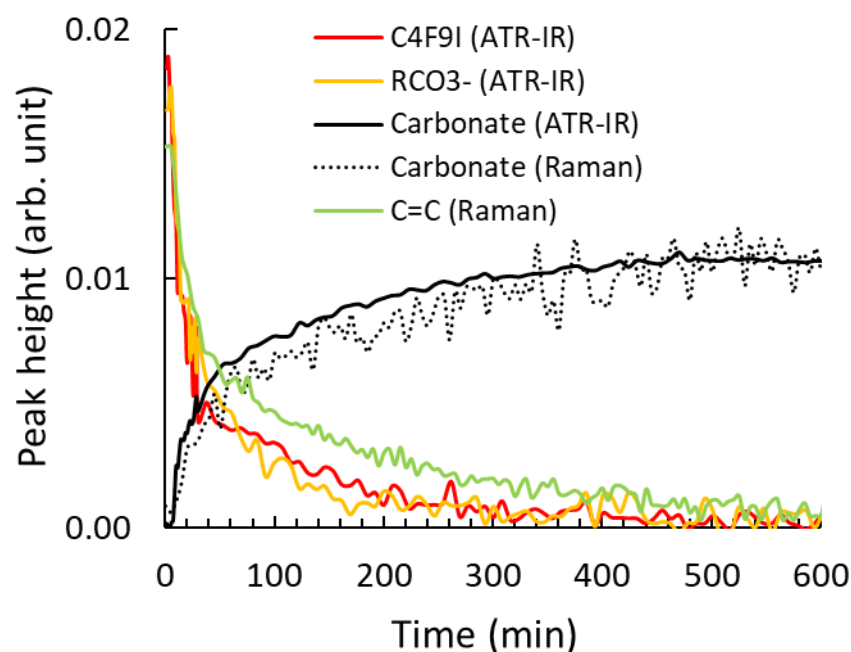
Figure 2. Kinetic profiles followed on the same model reaction by ATR-IR and Raman spectroscopies. The kinetics were recorded once the LED (365 nm) was switched on, i.e., 5 min after the solution containing allyl alcohol (0.5 mmol), DBU (1.05 equiv.), C_4F_9I (1.25 equiv.), and CO_2 (0.3 MPa) in CH_3CN (1 mL) was prepared.

2.1.2. Effect of Reagent Stoichiometry

In order to investigate the influence of the stoichiometry of DBU and C_4F_9I on the reaction outcome, in situ ATR-IR kinetic studies of the photoinduced carboxylative coupling of CO_2 with allyl alcohol were performed.

Fixing the amount of C_4F_9I (1.25 equiv.), the quantity of DBU was varied from 0.5 to 1.5 equiv. (see Figure 3). While increasing the amount of DBU from 0.5 to 1.5 equiv. did not affect the initial reaction rates, lower yields of **1** were obtained when deviating from the optimal amount of about 1–1.05 equiv. Using 0.5 and 0.75 equiv. of DBU led to decreased yields of **1** by about 55% and 20%, respectively. This is what is expected when considering the mechanism of Scheme 1 in which the DBU combined with CO_2, first reacts quickly and quantitatively in the dark with allyl alcohol to generate the allyl carbonate/DBUH$^+$ ion pair, which then, under light irradiation, undergoes the ATRA reaction followed by intramolecular cyclization to deliver **1** and DBUH$^+$/I$^-$. More surprising is the detrimental effect on the yield when using an excess of DBU, the decrease in the **1** yield of ~10% and 20% with 1.25 and 1.5 equiv. of DBU, respectively. In agreement with our previous study [52], this could be ascribed to the side reactivity of DBU with RfI, most probably to generate DBUC$_4$F$_9$H$^+$-I$^-$. This would ultimately lead to the consumption of a significant amount of RfI.

Then, using a slight excess amount of DBU (1.05 equiv.), we varied the quantity of C_4F_9I from 1 to 1.5 equiv. (see Figure 4). Although a barely detected improvement of the yield was observed upon an increase in the amount of C_4F_9I from 1 to 1.25, a further increase in the amount of C_4F_9I up to 1.5 equiv. had a detrimental effect on the yield. Finally, using 1 equiv. of DBU and 1 equiv. of C_4F_9I led to a significantly reduced yield.
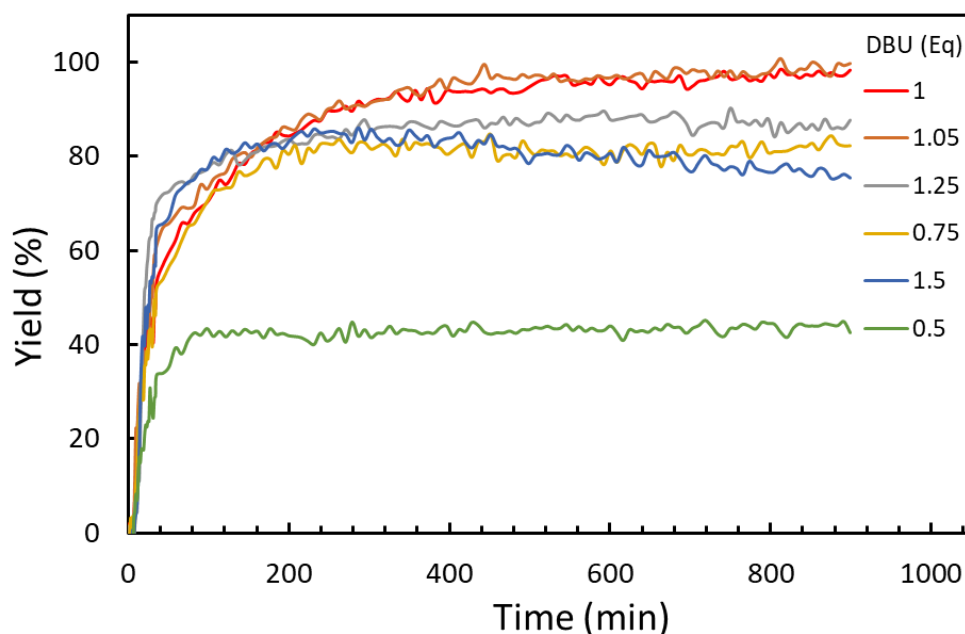
Figure 3. Influence of the amount of DBU on the rate of formation and yield of carbonate **1** followed in situ by ATR-IR spectroscopy. Conditions: allyl alcohol (48 μL, 0.5 mmol), DBU (0.5–1.5 equiv.), C_4F_9I (1.25 equiv.), CH_3CN (1 mL), 25 °C, CO_2 (0.3 MPa), $h\nu$ = 365 nm (LED).
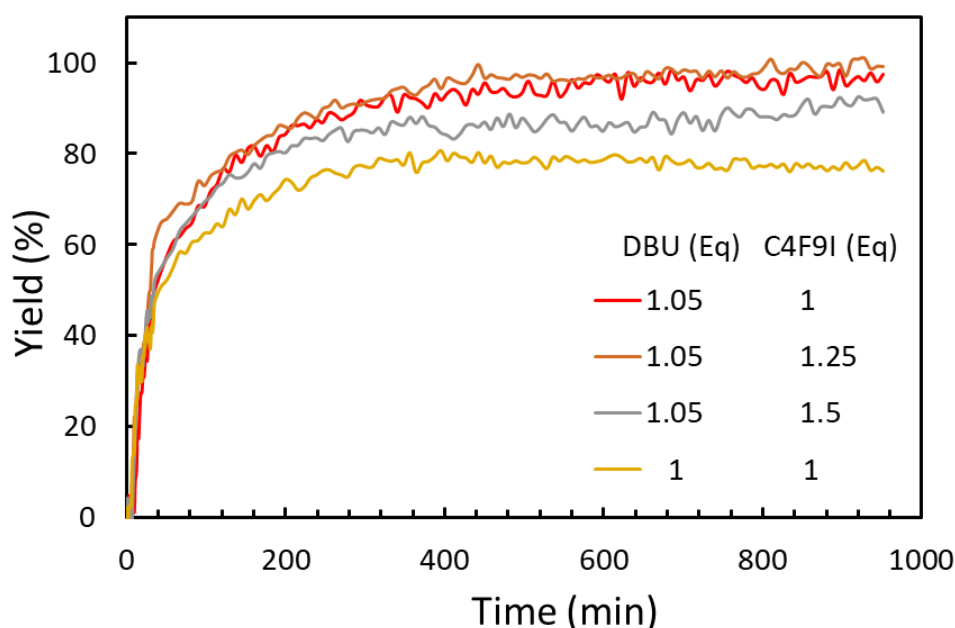

Figure 4. Influence of the amount of C_4F_9I on the kinetic of formation of perfluorobutyl carbonate followed by in situ ATR-IR spectroscopy. Conditions: allyl alcohol (48 μL, 0.5 mmol), DBU (1.05–1 equiv.), C_4F_9I (1–1.5 equiv.), CH_3CN (1 mL), 25 °C, CO_2 (0.3 MPa), $h\nu$ = 365 nm (LED).

Therefore, to further investigate our model reaction, we used an excess amount of DBU (1.05 equiv.) and C_4F_9I (1.25 equiv.) for which we obtained the maximum yield.

2.1.3. Halogen Bonding Effect

The presence of DBU is mandatory in order to deprotonate allyl alcohol in the presence of CO_2 to form the allyl carbonate anion. We also recently showed that DBU could form a halogen bond with RfI [52], thus potentially weakening the Rf−I bond, but also that the UV absorption of the [RfI-DBU] halogen bond complex was enhanced and red-shifted

compared to that of RfI, thus facilitating the direct photolysis of the Rf−I bond to generate Rf radicals which initiate a radical chain process [53]. In order to verify that halogen bonding is playing a key role for the ATRA reaction, we first performed a reaction without DBU. The follow-up of the reaction displayed in Figure 5 revealed that the peak height of C_4F_9I at 684 cm^{-1} was constant over time, hence showing that C_4F_9I was not consumed during the reaction, confirming that DBU plays a crucial role in the ATRA process. A reaction was then performed using allyl benzene as a substrate in the presence of a catalytic amount of DBU, i.e., 10 mol%. Allyl benzene was chosen in order to avoid the presence of the hydroxyl group on the substrate as well as the carbonatation step promoted by DBU and leading to its protonation. As seen in Figure 5, when a catalytic amount of DBU is used, a fast consumption of C_4F_9I is observed, i.e., ~50% in 40 min, while full consumption is achieved in about 5 h. Therefore, as reported before [52], DBU catalyzes the light-promoted iodoperfluoroalkylation reaction, most likely due to a halogen bond interaction with C_4F_9I. Thus, in the photo-induced carboxylative cyclization reaction, the Bronsted and Lewis basicities of DBU are both playing a key role.
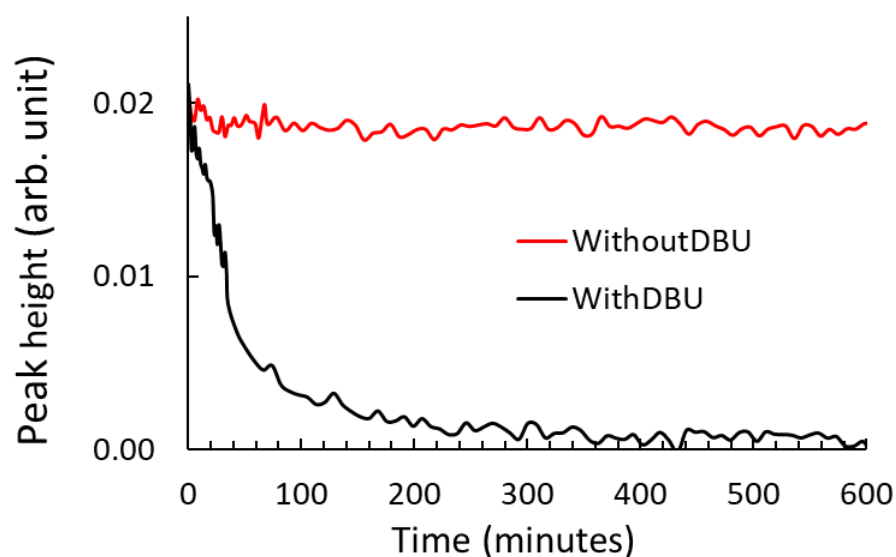

Figure 5. Evolution of the height of the peak at 684 cm^{-1} of C_4F_9I in the presence of DBU (with allyl benzene) or without DBU (with ally alcohol) followed by in situ ATR-IR spectroscopy. Conditions: allyl alcohol or allyl benzene (0.5 mmol) without DBU or DBU (0.1 equiv.), respectively, C_4F_9I (1.25 equiv.), CH_3CN (1 mL), 25 °C, CO_2 (0.3 MPa), $h\nu$ = 365 nm (LED).

2.1.4. Lewis Base Effect

The influence of the nature of the base, i.e., the tertiary amines (TEA, TMEDA, DABCO) and guanidines (TMG, MTBD), was then studied on the model reaction (see Figure 6). In comparison with the reference amidine (DBU), the acyclic guanidine (TMG) shows similar reactivity, although the rate of formation of the cyclic carbonate with TMG is significantly faster. A fast initial rate is also observed with the cyclic guanidine MTBD, but the reaction stops at ~65%. This could be ascribed to secondary reactions such as the nucleophilic attack of the allyl alcohol to **1** that that was shown to occur in the MTBD-catalyzed coupling of 2-methyl-3-butyn-2-ol with CO_2 [20]. Alternatively, the strong absorption of the MTBD-RfI halogen bonded complex in the UVA spectral range as reported in reference [52] could be responsible for secondary photochemical reactions that would ultimately lead to the consumption of a significant amount of RfI.
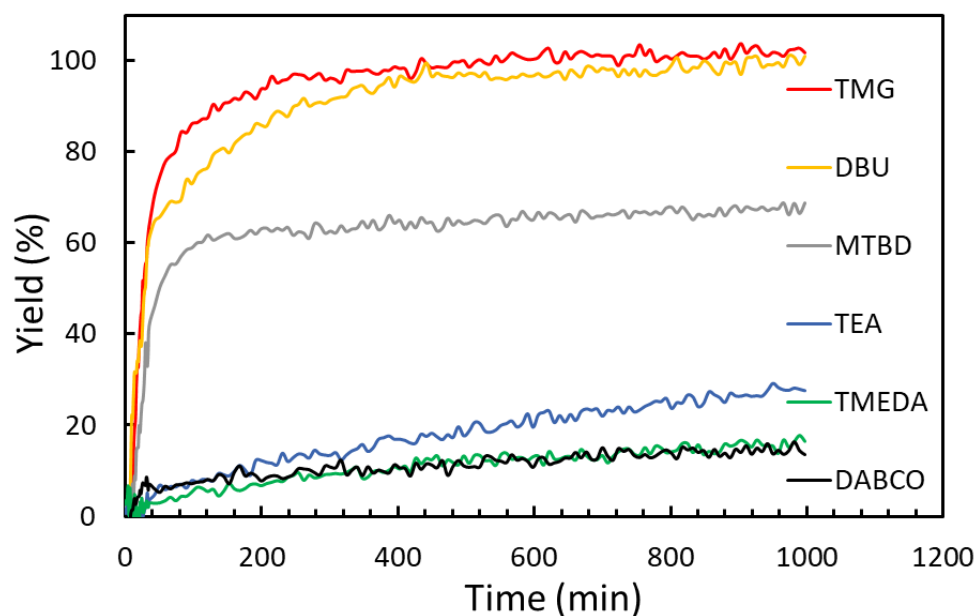
Figure 6. Influence of the nature of the base on the kinetic of formation of perfluorobutyl carbonate followed by in situ ATR-IR spectroscopy. Conditions: allyl alcohol (48 µL, 0.5 mmol), base (1.05 equiv.), C_4F_9I (1.25 equiv.), CH_3CN (1 mL), 25 °C, CO_2 (0.3 MPa), $h\nu$ = 365 nm (LED).

Using tertiary amines, the reaction proceeds at a very slow rate, the yields of cyclic carbonate after 15 h reaching only ~25% with TEA and ~15% with TMEDA and DABCO. Therefore, it appears that although strong (Brønsted/Lewis) bases are needed in order to reach high yields for such reaction, TMG and DBU display higher selectivity towards the synthesis of **1**.

2.1.5. Mechanism

Thus, from the experimental results obtained above, a plausible mechanism for the photoinduced carboxylative coupling of CO_2 with allyl alcohol is depicted in Scheme 3.
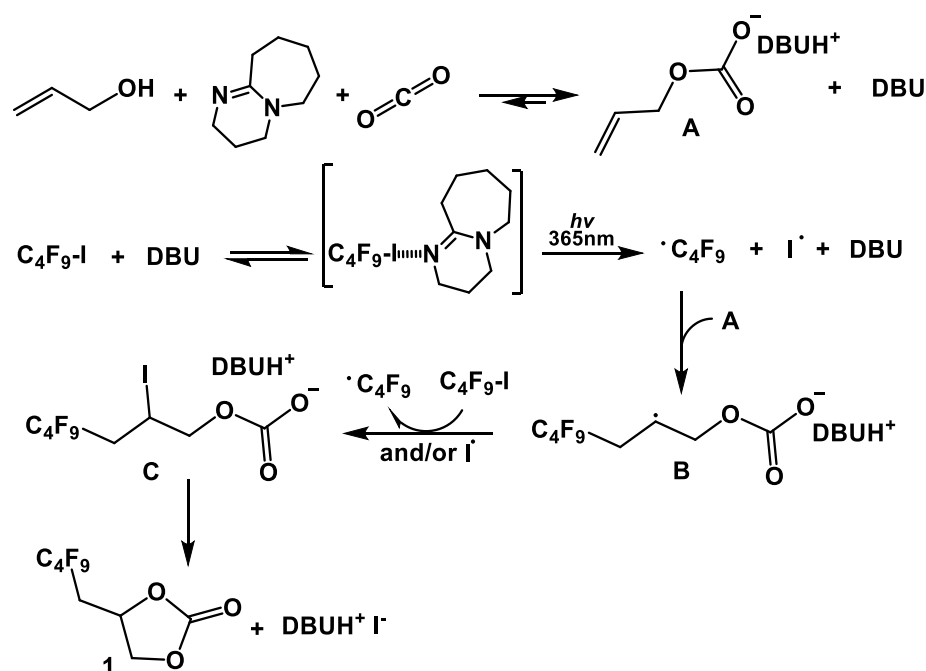
Scheme 3. Mechanism proposal for the formation of the perfluorobutyl carbonate **1**.

The first step, which occurs in the dark during the preparation of the reaction mixture, is the carbonation of the alcohol group that leads to the carbonate **A** along with unreacted DBU (~10%). When the LED is switched on, the CF_2–I bond activated by DBU through a halogen bond undergoes a homolytic cleavage to generate I• and C_4F_9• radicals, the latter adding onto carbonate **A** to provide the radical intermediate **B**. **B** could then react with I• or, more likely, abstract the iodine atom of C_4F_9I to afford the iodocarbonate **C** and C_4F_9• which propagates a radical chain process. Finally, the fast intramolecular cyclization affords the cyclic carbonate **1** along with $DBUH^+ I^-$.

2.2. Influence of Experimental Parameters

Considering the model reaction using allyl alcohol, 1.05 equiv. DBU and 1.25 equiv. C_4F_9I, the influence of different reaction conditions on kinetics and yields for the formation of perfluorobutyl cyclic carbonate were investigated including the temperature, the pressure, the irradiation wavelength and the nature of the solvent.

2.2.1. Temperature and Pressure Effect

The influence of the temperature on the kinetics and yields is illustrated in Figure 7. At a fixed pressure of 0.3 MPa, the temperature increase from 25 °C to 50 °C did not affect the reaction significantly. In contrast, heating up to 70 °C led to a maximum yield of about 30%. This agrees with the previous works that showed that the carbonation of alcohols promoted by a super base such as DBU is exothermic and highly effective at room temperature, and that heating at 90 °C shifts the equilibrium towards the starting reactants [51,54].
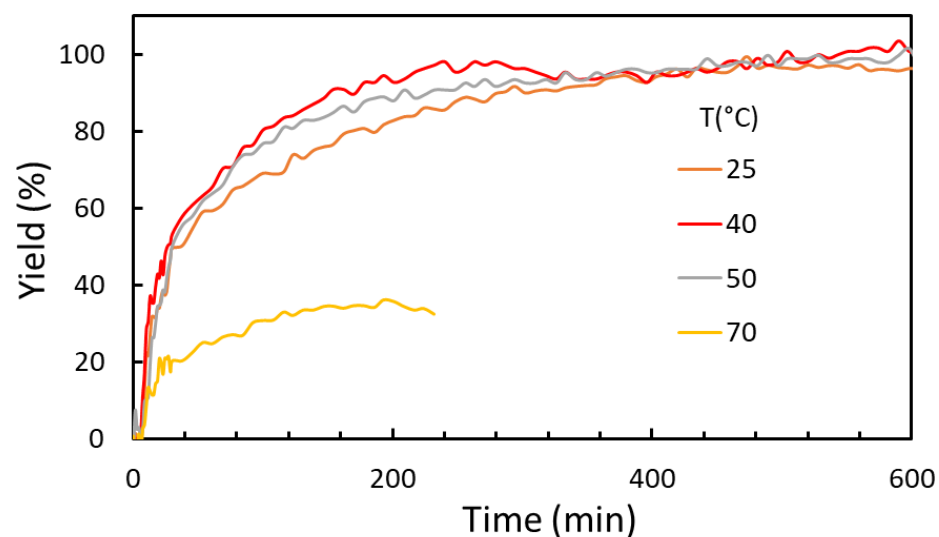

Figure 7. Influence of temperature on the kinetic of formation of **1** followed by in situ ATR-IR spectroscopy. Conditions: allyl alcohol (48 µL, 0.5 mmol), DBU (1.05 equiv.), C_4F_9I (1.25 equiv.), CH_3CN (1 mL), T (25, 40, 50, 70 °C), CO_2 (0.3 MPa), $h\nu$ = 365 nm (LED).

Similar rates and yields were obtained when conducting the reaction at 0.15, 0.35 and 2 MPa (see Figure 8). Thus, using DBU, the reaction proceeds very effectively in the presence of slight excess of the base with respect to allyl alcohol and at low CO_2 pressure. In agreement with Heldebrant's work and the results of this study, the alcohol group predominantly exists in the form of a carbonate in the reaction conditions, which ensures a highly effective carboxylative cyclization compared to the possible competitive epoxidation from the iodoperfluoroalkyl alcohol.
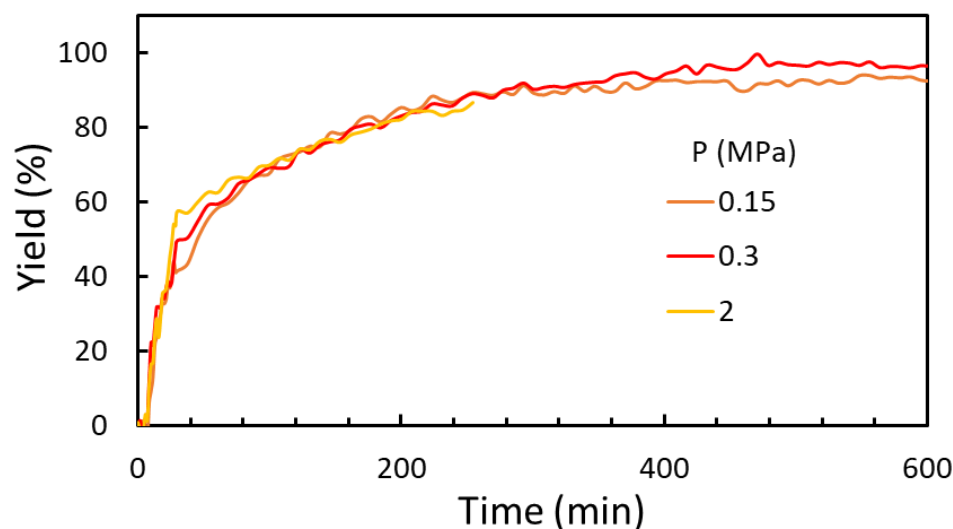
Figure 8. Influence of pressure of CO_2 on the kinetic of formation of **1** followed by in situ ATR-IR spectroscopy. Conditions: allyl alcohol (48 µL, 0.5 mmol), DBU (1.05 equiv.), C_4F_9I (1.25 equiv.), CH_3CN (1 mL), T = 25 °C, CO_2 (0.15, 0.3, 2 MPa), $h\nu$ = 365 nm (LED).

2.2.2. Irradiation Wavelength Effect

The effect of the irradiation wavelength on the kinetic and yield of the reaction have been studied using a UVA LED (365 nm), a blue LED (405 nm) and a white light LED (425–700 nm). As shown in Figure 9, the UVA and blue light irradiation led to similar reaction rates and yields while white light irradiation (>425 nm) led to a slower rate and moderate yield (~60%) in 10 h. Thus, due to the formation of the halogen bond complex [C_4F_9I-DBU] whose absorption tails up to the blue region of the optical spectrum [52], rather low energy blue photons promote the homolytic cleavage of the C_4F_9-I bond to generate Rf•, which initiates a radical chain process.
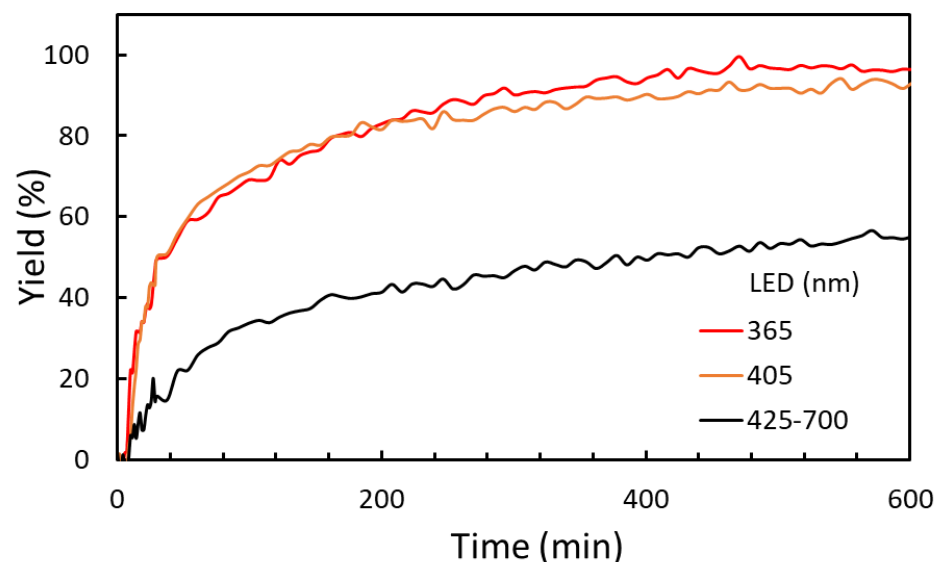

Figure 9. Influence of the irradiation wavelength on the kinetic of formation of **1** followed by in situ ATR-IR spectroscopy. Conditions: allyl alcohol (48 µL, 0.5 mmol), DBU (1.05 equiv.), C_4F_9I (1.25 equiv.), CH_3CN (1 mL), T = 25 °C, CO_2 (0.3 MPa), $h\nu$ = 365 nm, 405 nm and 425–700 nm (LED).

2.2.3. Solvent Effect

The influence of the nature of the solvent on the kinetics and the yields of the reaction was then evaluated with various organic solvents such as THF, DMSO and anisole, the latter being a biobased solvent [55]. Although CH_3CN appears to be the best solvent for

this reaction in terms of kinetics and yield, the perfluorobutyl carbonate **1** could be formed in a good yield (~85%) using DMSO (see Figure 10). Lower yields of about 60 and 30% were obtained with THF and anisole, respectively.
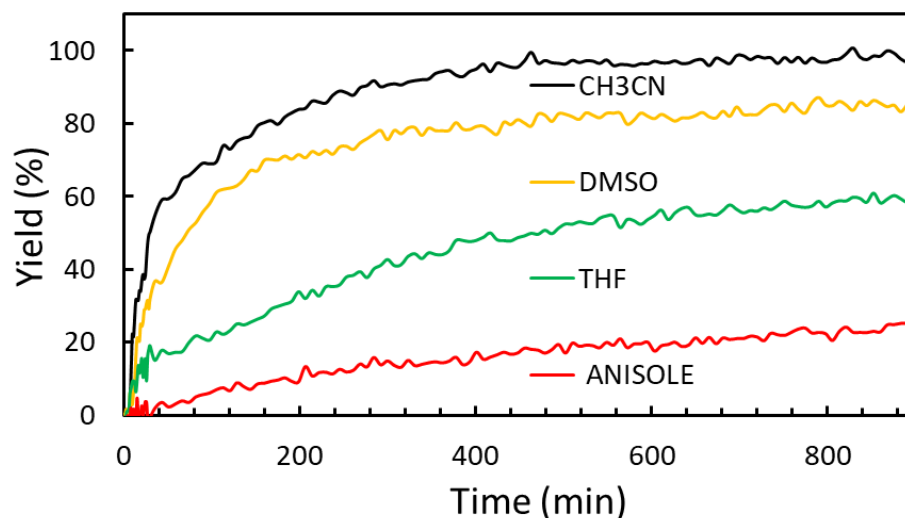

Figure 10. Influence of the solvent on the kinetic of formation of **1** followed by in situ ATR-IR spectroscopy. Conditions: allyl alcohol (48 μL, 0.5 mmol), DBU (1.05 equiv.), C_4F_9I (1.25 equiv.), solvent (1 mL), T = 25 °C, CO_2 (0.3 MPa), $h\nu$ = 365 nm (LED).

2.3. Substrate Scope

In an effort to extend the applicability of the protocol used for the synthesis of perfluorobutyl carbonate, several commercially available allylic and propargylic alcohols were tested for the formation of both five- and six-membered cyclic carbonates (Scheme 4).
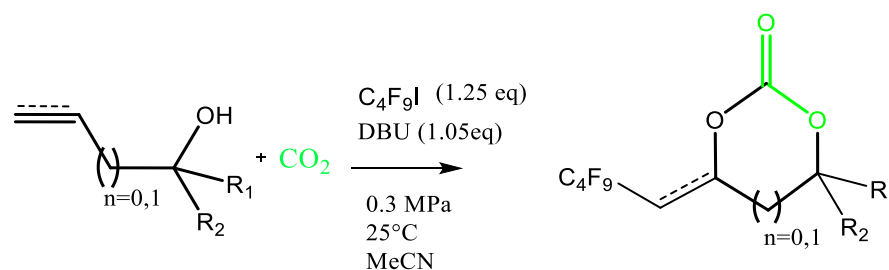
Scheme 4. Substrate scope using optimal conditions of the model reaction.

Figure 11 shows the time dependence of the formation of five- and six-membered cyclic carbonates from various alcohols. Allylic alcohols such as 1-pentene-3-ol, crotyl alcohol and geraniol were converted into five-membered cyclic carbonates but in lower yield than that obtained for allyl alcohol. No cyclic carbonate was formed from the tertiary allylic alcohol 2-methyl 3 butene-2-ol. Contrasting with other alcohols, the alkyl carbonate anion $RCO_3{}^-$ did not form upon the addition of CO_2 at a pressure of 0.3 MPa. Interestingly, it was possible to convert 3-butene-1-ol into a six-membered cyclic carbonate, albeit in a lower IR yield compared to allyl alcohol. Finally, propargyl alcohol could not be converted into any five-membered cyclic carbonate. This is probably due to the fact that the intramolecular nucleophilic substitution on an sp2 carbon is more difficult to achieve.
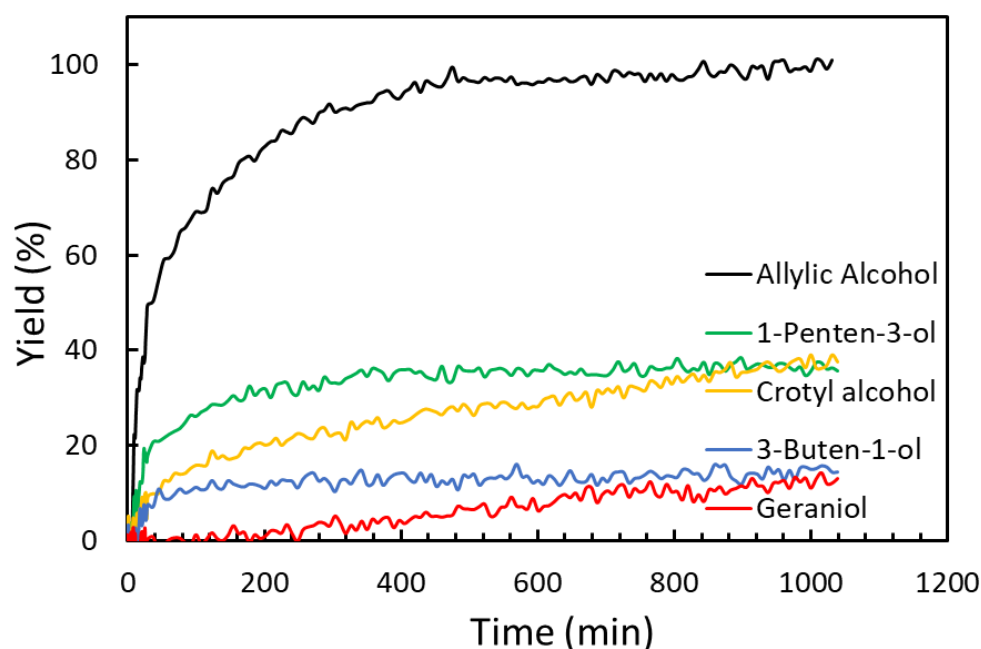
Figure 11. Kinetic investigation of the substrate scope to afford 5- and 6-membered perfluorobutyl cyclic carbonate. Conditions: substrate (0.5 mmol), base (1.05 equiv.), C_4F_9I (1.25 equiv.), CH_3CN (1 mL), 25 °C, CO_2 (0.3 MPa), $h\nu$ = 365 nm (LED).

3. Materials and Methods

3.1. Material

Allyl alcohol (Sigma Aldrich, St. Louis, MO, USA), 1-pentene-3-ol (Sigma Aldrich), Crotyl alcohol (Sigma Aldrich), Geraniol (Sigma Aldrich), 3-butene-1-ol (Sigma Aldrich), 2-methyl 3 butene-2-ol (Sigma Aldrich), propargyl alcohol (Sigma Aldrich), acetonitrile (CH_3CN, Sigma Aldrich), dimethyl sulfoxide (DMSO, Sigma Aldrich), tetrahydrofuran (THF, Sigma Aldrich), Anisole (Alfa Aesar, Haverhill, MA, USA), 1,8-diazabicyclo[5.4.0]undec-7-ene (DBU, Alfa Aesar), triethylamine (Et_3N, Sigma Aldrich), 7-Methyl-1,5,7-Triazabicyclo [4.4.0]dec-5-ene (MTBD, Sigma Aldrich), TetramethylGuanidine (TMG, Alfa Aesar), Tetramethylethylenediamine, (TMEDA, Sigma Aldrich), 1,4-Diazabicyclo[2.2.2]octane (DABCO, Sigma Aldrich) and Perfluorobutyl iodide (C_4F_9I, Sigma Aldrich) were used without further purification.

3.2. In Situ Kinetics Methods

The reactions were monitored in situ by ATR-IR spectroscopy using a homemade Ge ATR accessory suitable for high-pressure measurements (up to 5 MPa) and high temperature (up to 100 °C) (see ESI, Figure S2) coupled with a ThermoOptek interferometer (type 6700) equipped with a globar source, a KBr/Ge beamsplitter and a DTGS (Deuterated TriGlycine Sulphate) detector. Single-beam spectra recorded in the spectral range (600–4000 cm^{-1}) with a 4 cm^{-1} resolution were obtained after the Fourier transformation of 20 accumulated interferograms for the first 20 spectra (one spectrum every 80 s), and then Fourier transformation of 120 accumulated interferograms until the end of reaction time (one spectrum every 8 min) was also performed.

The in situ Raman scattering investigations were performed using a Jobin-Yvon Horiba XploRA confocal Raman microscope equipped with a 10× objective and a laser diode at a wavelength λ = 785 nm and a 100% laser power of 45 mW. The spectral range from 140 to 2600 cm^{-1} was recorded with a grating of 600 L/mm and a resolution of about 5 cm^{-1}. The spectra resulted from two acquisitions of 20 s each to improve the signal-to-noise ratio. A homemade high-pressure cell (up to 10 MPa with a volume of 3 mL) equipped with two sapphire windows was used in order to simultaneously measure the Raman spectra and irradiate the mixture with the same LED as that used on the ATR-IR set-up.

The LEDs used in this study were purchased from Thorlabs. The LED at 365 nm (M365FP1) used for most of the experiments delivers an irradiance of about 5 mW/cm^2 on the sample. Two other LEDS, M405FP1 (405 nm) and MWWHF2 (425–700 nm), were used for comparison at the same irradiance (5 mW/cm^2).

The alcohol (0.5 mmol) was solubilized in a 2 mL vial with 1 mL of solvent. C$_4$F$_9$I (1.25 equiv.) was added to the vial, and then the Lewis base (1.05 equiv.) was added to the vial. The whole mixture was then transferred to the reaction chamber (volume: 5 mL) which was directly fixed on the Ge crystal of the ATR-IR device and on which a sapphire window allows the irradiation of the mixture with a LED. The mixture was constantly homogenized during the experiment using a magnetically driven stirrer disposed in the reaction chamber. An optical lens was connected to the sapphire window's support and the LED was connected to the optical lens via an optical fibre in order to ensure a good reproducibility for the irradiation of all the mixtures investigated. The setup was sealed with the CO$_2$ feed pipe. The first spectrum was recorded, and then, once CO$_2$ was introduced in the sample chamber at the desired pressure, the kinetic was started. A few minutes later, the LED was switched on in order to start the photoinduced carboxylative coupling of CO$_2$ with various alcohols. At the end of the reaction, in order to determine the yield, the ATR-IR spectrum of the reaction mixture was compared with the corresponding spectrum of the neat carbonate recorded under the same conditions. The absorbance (A (1810)) of the peak associated to the ν(C=O) stretching mode at 1810 cm^{-1} of the cyclic carbonate was used to determine the yield for the entire kinetic deduced by proportionality according to Equation (1). A number of experiments were conducted at least twice in order to check for reproducibility. We emphasize that ATR-IR spectroscopy can be considered a quantitative method like ^{1}H NMR as demonstrated in our previous work [40] with an accuracy of about ±3% and can highlight the potential formation of by-products.

$$Yield\ (\%) = \frac{[A(t)(1810)](\text{reaction mixture})}{[A\ (1810)](\text{neat carbonate})}. \tag{1}$$

4. Conclusions

In this paper, we investigated an original protocol for the synthesis of perfluoroalkylated cyclic carbonate by the photoinduced carboxylative cyclization of allyl alcohols with CO$_2$ promoted by visible/UVA light irradiation using perfluoroalkyl iodides. Under optimized conditions, quantitative yields up to 99% in perfluorobutyl carbonate were reached in less than 8 h at 298 K and 0.15 MPa under blue irradiation at 405 nm. In situ kinetic studies by ATR-IR and Raman spectroscopy revealed the evolution of all the components of the complex mixture during the reaction while varying key parameters such as the stoichiometry of the reactants, the nature of the Lewis base, the temperature, the pressure, the irradiation wavelength, the solvent and the substrate scope. Such fundamental kinetic studies enabled the determination of the reaction mechanism and provided insight into the underlying reason for the observed kinetics and selectivity. In particular, it was found that strong Lewis bases are needed that play both the role of activating the allyl alcohol for the generation of the allyl carbonate in the presence of CO$_2$ and promoting the ATRA reaction through the activation of C$_4$F$_9$I by halogen bonding. Various allylic alcohols such has 1-pentene-3-ol, crotyl alcohol and geraniol (a biobased substrate) were converted into five-membered cyclic carbonates. Interestingly, it was possible to convert 3-butene-1-ol into a six-membered cyclic carbonate although to a lower yield. Thus, this route offers a sustainable and promising approach for the valorisation of CO$_2$ as a chemical feedstock through efficient usage of light energy.

References

1. North, M.; Pasquale, R.; Young, C. Synthesis of cyclic carbonates from epoxides and CO_2. *Green Chem.* **2010**, *12*, 1514–1539. [CrossRef]
2. Cokoja, M.; Wilhelm, M.E.; Anthofer, M.H.; Herrmann, W.A.; Kühn, F.E. Synthesis of Cyclic Carbonates from Epoxides and Carbon Dioxide by Using Organocatalysts. *ChemSuschem* **2015**, *8*, 2436–2454. [CrossRef] [PubMed]
3. Gennen, S.; Alves, M.; Méreau, R.; Tassaing, T.; Gilbert, B.; Detrembleur, C.; Jerome, C.; Grignard, B. Fluorinated Alcohols as Activators for the Solvent-Free Chemical Fixation of Carbon Dioxide into Epoxides. *ChemSuschem* **2015**, *8*, 1845–1849. [CrossRef] [PubMed]
4. Alves, M.; Grignard, B.; Gennen, S.; Mereau, R.; Detrembleur, C.; Jerome, C.; Tassaing, T. Organocatalytic promoted coupling of carbon dioxide with epoxides: A rational investigation of the cocatalytic activity of various hydrogen bond donors. *Catal. Sci. Technol.* **2015**, *5*, 4636–4643. [CrossRef]
5. Alves, M.; Grignard, B.; Mereau, R.; Jerome, C.; Tassaing, T.; Detrembleur, C. Organocatalyzed coupling of carbon dioxide with epoxides for the synthesis of cyclic carbonates: Catalyst design and mechanistic studies. *Catal. Sci. Technol.* **2017**, *7*, 2651–2684. [CrossRef]
6. Shaikh, A.-A.G.; Sivaram, S. Organic carbonates. *Chem. Rev.* **1996**, *96*, 951–976. [CrossRef]
7. Tempelaar, S.; Mespouille, L.; Coulembier, O.; Dubois, P.; Dove, A.P. Synthesis and post-polymerisation modifications of aliphatic poly(carbonate)s prepared by ring-opening polymerisation. *Chem. Soc. Rev.* **2013**, *42*, 1312–1336. [CrossRef]
8. Grignard, B.; Gennen, S.; Jérôme, C.; Kleij, A.W.; Detrembleur, C. Advances in the use of CO_2 as a renewable feedstock for the synthesis of polymers. *Chem. Soc. Rev.* **2019**, *48*, 4466–4514. [CrossRef]
9. Maisonneuve, L.; Lamarzelle, O.; Rix, E.; Grau, E.; Cramail, H. Isocyanate-Free Routes to Polyurethanes and Poly(hydroxy Urethane)s. *Chem. Rev.* **2015**, *115*, 12407–12439. [CrossRef]
10. Grignard, B.; Thomassin, J.M.; Gennen, S.; Poussard, L.; Bonnaud, L.; Raquez, J.M.; Dubois, P.; Tran, M.P.; Park, C.B.; Jerome, C.; et al. CO_2-blown microcellular non-isocyanate polyurethane (NIPU) foams: From bio- and CO_2-sourced monomers to potentially thermal insulating materials. *Green Chem.* **2016**, *18*, 2206–2215. [CrossRef]
11. Gennen, S.; Grignard, B.; Tassaing, T.; Jérôme, C.; Detrembleur, C. CO_2-Sourced α-Alkylidene Cyclic Carbonates: A Step Forward in the Quest for Functional Regioregular Poly(urethane)s and Poly(carbonate)s. *Angew. Chem. Int. Ed.* **2017**, *56*, 10394–10398. [CrossRef]
12. Monie, F.; Grignard, B.; Thomassin, J.-M.; Mereau, R.; Tassaing, T.; Jerome, C.; Detrembleur, C. Chemo- and Regioselective Additions of Nucleophiles to Cyclic Carbonates for the Preparation of Self-Blowing Non-Isocyanate Polyurethane Foams. *Angew. Chem. Int. Ed.* **2020**, *59*, 17033–17041. [CrossRef]
13. Martín, C.; Fiorani, G.; Kleij, A.W. Recent Advances in the Catalytic Preparation of Cyclic Organic Carbonates. *ACS Catal.* **2015**, *5*, 1353–1370. [CrossRef]
14. Rintjema, J.; Guo, W.; Martin, E.; Escudero-Adan, E.C.; Kleij, A.W. Highly Chemoselective Catalytic Coupling of Substituted Oxetanes and Carbon Dioxide. *Chemistry* **2015**, *21*, 10754–10762. [CrossRef]
15. Alves, M.; Grignard, B.; Boyaval, A.; Méreau, R.; De Winter, J.; Gerbaux, P.; Detrembleur, C.; Tassaing, T.; Jérôme, C. Organocatalytic Coupling of CO_2 with Oxetane. *ChemSuschem* **2017**, *10*, 1128–1138. [CrossRef]
16. Besse, V.; Camara, F.; Voirin, C.; Auvergne, R.; Caillol, S.; Boutevin, B. Synthesis and applications of unsaturated cyclocarbonates. *Polym. Chem.* **2013**, *4*, 4545–4561. [CrossRef]
17. Zhao, Y.; Yang, Z.; Yu, B.; Zhang, H.; Xu, H.; Hao, L.; Han, B.; Liu, Z. Task-specific ionic liquid and CO_2-cocatalysed efficient hydration of propargylic alcohols to [small alpha]-hydroxy ketones. *Chem. Sci.* **2015**, *6*, 2297–2301. [CrossRef]
18. Song, Q.-W.; He, L.-N. *Advances in CO_2 Capture, Sequestration, and Conversion*; American Chemical Society: Washington, DC, USA, 2015; Volume 1194, Chapter 2; pp. 47–70.

19. Rintjema, J.; Kleij, A.W. Substrate-Assisted Carbon Dioxide Activation as a Versatile Approach for Heterocyclic Synthesis. *Synthesis* **2016**, *48*, 3863–3878. [CrossRef]

20. Boyaval, A.; Méreau, R.; Grignard, B.; Detrembleur, C.; Jerome, C.; Tassaing, T. Organocatalytic Coupling of CO_2 with a Propargylic Alcohol: A Comprehensive Mechanistic Study. *ChemSuschem* **2017**, *10*, 1241–1248. [CrossRef]

21. Li, M.; Abdolmohammadi, S.; Hoseininezhad-Namin, M.S.; Behmagham, F.; Vessally, E. Carboxylative cyclization of propargylic alcohols with carbon dioxide: A facile and Green route to α-methylene cyclic carbonates. *J. CO2 Util.* **2020**, *38*, 220–231. [CrossRef]

22. Huang, J.; Jehanno, C.; Worch, J.C.; Ruipérez, F.; Sardon, H.; Dove, A.P.; Coulembier, O. Selective Organocatalytic Preparation of Trimethylene Carbonate from Oxetane and Carbon Dioxide. *ACS Catal.* **2020**, *10*, 5399–5404. [CrossRef]

23. Méreau, R.; Grignard, B.; Boyaval, A.; Detrembleur, C.; Jerome, C.; Tassaing, T. Tetrabutylammonium Salts: Cheap Catalysts for the Facile and Selective Synthesis of α-Alkylidene Cyclic Carbonates from Carbon Dioxide and Alkynols. *ChemCatChem* **2018**, *10*, 956–960. [CrossRef]

24. Grignard, B.; Ngassamtounzoua, C.; Gennen, S.; Gilbert, B.; Méreau, R.; Jerome, C.; Tassaing, T.; Detrembleur, C. Boosting the Catalytic Performance of Organic Salts for the Fast and Selective Synthesis of α-Alkylidene Cyclic Carbonates from Carbon Dioxide and Propargylic Alcohols. *ChemCatChem* **2018**, *10*, 2584–2592. [CrossRef]

25. Dabral, S.; Bayarmagnai, B.; Hermsen, M.; Schießl, J.; Mormul, V.; Hashmi, A.S.K.; Schaub, T. Silver-Catalyzed Carboxylative Cyclization of Primary Propargyl Alcohols with CO_2. *Org. Lett.* **2019**, *21*, 1422–1425. [CrossRef] [PubMed]

26. Cervantes-Reyes, A.; Saxl, T.; Stein, P.M.; Rudolph, M.; Rominger, F.; Asiri, A.M.; Hashmi, A.S.K. Expanded Ring NHC Silver Carboxylate Complexes as Efficient and Reusable Catalysts for the Carboxylative Cyclization of Unsubstituted Propargylic Derivatives. *ChemSuschem* **2021**, *14*, 2367–2374. [CrossRef]

27. Cervantes-Reyes, A.; Farshadfar, K.; Rudolph, M.; Rominger, F.; Schaub, T.; Ariafard, A.; Hashmi, A.S.K. Copper-catalysed synthesis of α-alkylidene cyclic carbonates from propargylic alcohols and CO_2. *Green Chem.* **2021**, *23*, 889–897. [CrossRef]

28. Kindermann, N.; Jose, T.; Kleij, A.W. Synthesis of Carbonates from Alcohols and CO_2. *Top Curr Chem.* **2017**, *375*, 15. [CrossRef]

29. Tamura, M.; Honda, M.; Nakagawa, Y.; Tomishige, K. Direct conversion of CO_2 with diols, aminoalcohols and diamines to cyclic carbonates, cyclic carbamates and cyclic ureas using heterogeneous catalysts. *J. Chem. Technol. Biotechnol.* **2014**, *89*, 19–33. [CrossRef]

30. Hosseinian, A.; Farshbaf, S.; Mohammadi, R.; Monfared, A.; Vessally, E. Advancements in six-membered cyclic carbonate (1,3-dioxan-2-one) synthesis utilizing carbon dioxide as a C1 source. *RSC Adv.* **2018**, *8*, 17976–17988. [CrossRef]

31. Bobbink, F.D.; Gruszka, W.; Hulla, M.; Das, S.; Dyson, P.J. Synthesis of cyclic carbonates from diols and CO_2 catalyzed by carbenes. *Chem. Commun.* **2016**, *52*, 10787–10790. [CrossRef]

32. Brege, A.; Grignard, B.; Méreau, R.; Detrembleur, C.; Jerome, C.; Tassaing, T. En Route to CO_2-Based (a)Cyclic Carbonates and Polycarbonates from Alcohols Substrates by Direct and Indirect Approaches. *Catalysts* **2022**, *12*, 124. [CrossRef]

33. Honda, M.; Tamura, M.; Nakagawa, Y.; Tomishige, K. Catalytic CO_2 conversion to organic carbonates with alcohols in combination with dehydration system. *Catal. Sci. Technol.* **2014**, *4*, 2830–2845. [CrossRef]

34. Honda, M.; Tamura, M.; Nakao, K.; Suzuki, K.; Nakagawa, Y.; Tomishige, K. Direct Cyclic Carbonate Synthesis from CO_2 and Diol over Carboxylation/Hydration Cascade Catalyst of CeO_2 with 2-Cyanopyridine. *ACS Catal.* **2014**, *4*, 1893–1896. [CrossRef]

35. Reithofer, M.R.; Sum, Y.N.; Zhang, Y. Synthesis of cyclic carbonates with carbon dioxide and cesium carbonate. *Green Chem.* **2013**, *15*, 2086–2090. [CrossRef]

36. Mcguire, T.M.; López-Vidal, E.M.; Gregory, G.L.; Buchard, A. Synthesis of 5- to 8-membered cyclic carbonates from diols and CO2: A one-step, atmospheric pressure and ambient temperature procedure. *J. CO2 Util.* **2018**, *27*, 283–288. [CrossRef]

37. Gregory, G.L.; Ulmann, M.; Buchard, A. Synthesis of 6-membered cyclic carbonates from 1,3-diols and low CO_2 pressure: A novel mild strategy to replace phosgene reagents. *RSC Adv.* **2015**, *5*, 39404–39408. [CrossRef]

38. Kitamura, T.; Inoue, Y.; Maeda, T.; Oyamada, J. Convenient synthesis of ethylene carbonates from carbon dioxide and 1,2-diols at atmospheric pressure of carbon dioxide. *Synth. Commun.* **2015**, *46*, 39–45. [CrossRef]

39. Lim, Y.N.; Lee, C.; Jang, H.-Y. Metal-Free Synthesis of Cyclic and Acyclic Carbonates from CO_2 and Alcohols. *Eur. J. Org. Chem.* **2014**, *2014*, 1823–1826. [CrossRef]

40. Brege, A.; Méreau, R.; Mcgehee, K.; Grignard, B.; Detrembleur, C.; Jerome, C.; Tassaing, T. The coupling of CO_2 with diols promoted by organic dual systems: Towards products divergence via benchmarking of the performance metrics. *J. CO2 Util.* **2020**, *38*, 88–98. [CrossRef]

41. Baran, T.; Dibenedetto, A.; Aresta, M.; Kruczała, K.; Macyk, W. Photocatalytic Carboxylation of Organic Substrates with Carbon Dioxide at Zinc Sulfide with Deposited Ruthenium Nanoparticles. *ChemPlusChem* **2014**, *79*, 708–715. [CrossRef]

42. Masuda, Y.; Ishida, N.; Murakami, M. Light-Driven Carboxylation of o-Alkylphenyl Ketones with CO_2. *J. Am. Chem. Soc.* **2015**, *137*, 14063–14066. [CrossRef] [PubMed]

43. Wang, M.-Y.; Cao, Y.; Liu, X.; Wang, N.; He, L.-N.; Li, S.-H. Photoinduced radical-initiated carboxylative cyclization of allyl amines with carbon dioxide. *Green Chem.* **2017**, *19*, 1240–1244. [CrossRef]

44. Gui, Y.-Y.; Zhou, W.-J.; Ye, J.-H.; Yu, D.-G. Photochemical Carboxylation of Activated $C(sp^3)-H$ Bonds with CO_2. *ChemSuschem* **2017**, *10*, 1337–1340. [CrossRef]

45. Murata, K.; Numasawa, N.; Shimomaki, K.; Takaya, J.; Iwasawa, N. Construction of a visible light-driven hydrocarboxylation cycle of alkenes by the combined use of Rh(i) and photoredox catalysts. *Chem. Commun.* **2017**, *53*, 3098–3101. [CrossRef] [PubMed]

46. Long Ngo, H.; Kumar Mishra, D.; Mishra, V.; Chien Truong, C. Recent advances in the synthesis of heterocycles and pharmaceuticals from the photo/electrochemical fixation of carbon dioxide. *Chem. Eng. Sci.* **2021**, *229*, 116142. [CrossRef]
47. He, X.; Yao, X.Y.; Chen, K.H.; He, L.N. Metal-Free Photocatalytic Synthesis of exo-Iodomethylene 2-Oxazolidinones: An Alternative Strategy for CO_2 Valorization with Solar Energy. *ChemSuschem* **2019**, *12*, 5081–5085. [CrossRef] [PubMed]
48. Malik, A.; Bhatt, S.; Soni, A.; Khatri, P.K.; Guha, A.K.; Saikia, L.; Jain, S.L. Visible-light driven reaction of CO_2 with alcohols using a Ag/CeO_2 nanocomposite: First photochemical synthesis of linear carbonates under mild conditions. *Chem. Commun.* **2023**, *59*, 1313–1316. [CrossRef]
49. Heldebrant, D.J.; Jessop, P.G.; Thomas, C.A.; Eckert, C.A.; Liotta, C.L. The Reaction of 1,8-Diazabicyclo[5.4.0]undec-7-ene (DBU) with Carbon Dioxide. *J. Org. Chem.* **2005**, *70*, 5335–5338. [CrossRef]
50. Onwukamike, K.N.; Tassaing, T.; Grelier, S.; Grau, E.; Cramail, H.; Meier, M.A.R. Detailed Understanding of the DBU/CO_2 Switchable Solvent System for Cellulose Solubilization and Derivatization. *ACS Sustain. Chem. Eng.* **2018**, *6*, 1496–1503. [CrossRef]
51. Heldebrant, D.J.; Yonker, C.R.; Jessop, P.G.; Phan, L. Organic liquid CO_2 capture agents with high gravimetric CO_2 capacity. *Energy Environ. Sci.* **2008**, *1*, 487–493. [CrossRef]
52. Grondin, J.; Aupetit, C.; Vincent, J.-M.; Méreau, R.; Tassaing, T. Visible-light induced photochemistry of Electron Donor-Acceptor Complexes in Perfluoroalkylation Reactions: Investigation of halogen bonding interactions through UV–Visible absorption and Raman spectroscopies combined with DFT calculations. *J. Mol. Liq.* **2021**, *333*, 115993. [CrossRef]
53. Postigo, A. Electron Donor-Acceptor Complexes in Perfluoroalkylation Reactions. *Eur. J. Org. Chem.* **2018**, *2018*, 6391–6404. [CrossRef]
54. Smith, C.A.; Cramail, H.; Tassaing, T. Insights into the Organocatalyzed Synthesis of Urethanes in Supercritical Carbon Dioxide: An In Situ FTIR Spectroscopic Kinetic Study. *ChemCatChem* **2014**, *6*, 1380–1391. [CrossRef]
55. Prat, D.; Wells, A.; Hayler, J.; Sneddon, H.; Mcelroy, C.R.; Abou-Shehada, S.; Dunn, P.J. CHEM21 selection guide of classical- and less classical-solvents. *Green Chem.* **2016**, *18*, 288–296. [CrossRef]